THE EFFECT OF AREA RATIO ON THE OPTIMIZATION OF AN AC ELECTROSTATIC VIBRATION-TO-ELECTRICITY MICRO POWER GENERATOR

Yi Chiu*, Hung-Chih Liu
Department of Electrical Engineering, National Chiao Tung University, Hsin Chu, Taiwan, R.O.C.
*Presenting Author: yichiu@mail.nctu.edu.tw

Abstract: This paper presents the design and optimization of an AC electrostatic vibration-to-electricity micro generator under device area constraint. Since the output power increases with mass and capacitance, there is a trade-off between the areas occupied by the mass and the variable capacitors for a limited total device area. In this paper, we specifically investigate the effect of the area ratio on the device performance. It is found that large mass is favored over large capacitance in the pull-in limited operation. It is also found that maximum power can be generated for matched load. The optimal design of the AC micro generators with and without attached external mass is presented.

Keywords: energy harvesting, electrostatic, vibration, Simulink, pull-in, matched load

1. INTRODUCTION

Low power CMOS VLSI technology has enabled the development of applications such as wireless sensor networks or personal health monitoring. In these applications, lifetime and maintenance of the power supply is critical. Recently, energy scavenging from ambient natural sources, such as vibration and ambient heat, is attracting much interest as self-sustainable power sources. Among various approaches, electrostatic vibration-to-electricity conversion is promising due to its compatibility to IC processes and the ubiquity of vibration source in nature.

Electrostatic micro power generators can operate in DC or AC modes [1, 2]. In the DC (switched) mode, switches or diodes are used to control the timing of charge-discharge cycles of a vibration-driven variable capacitor so that a DC current flow through the converter and the load [2-4]. In the AC (continuous) mode, vibration causes a periodic variation of the capacitance and thus the charge on a biased variable capacitor. The varying charge represents an AC current and no switching devices are needed as in the DC-operated generators. The variable capacitor can be biased by an electret [5], the built-in voltage between two metals [6], a pre-charged capacitor [7], or simply a battery [2]. The inertial force on the generator and thus its output power increase with its mass. Therefore, an external mass can be attached to the generator to increase its output [2]. Output power also increases with the capacitance. As a result, it is usually desired to maximize both the mass and the capacitance. In a micro generator without the attached mass, however, there is a trade-off between the areas occupied by the mass and the variable capacitor for a limited total device area. In this paper, we specifically investigate the effect of the area ratio of the capacitance on the output power of the generators. A Simulink model was used to calculate the output of the generators for various design and operation parameters. Optimization of the generators with and without attached external mass is presented.

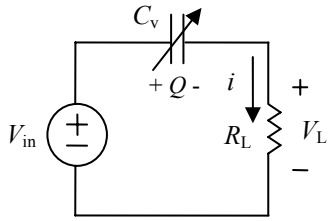

Fig. 1: Operation of an AC electrostatic generator.

Since the output power of a vibration-driven generator is related to the characteristics of the vibration source, a typical vibration of 2.25 m/s^2 at about 120 Hz, found in a number of household appliances, was used as the energy source in this paper.

2. PRINCIPLE AND ANALYSIS

The operation of the generator is shown in Figure 1 [1, 2]. The circuit is composed of an auxiliary power supply V_{in} such as a battery, a vibration-driven variable capacitor C_v and a load R_L connected in series with the capacitor. When the shuttle mass of the generator oscillates at the frequency of the vibration source, the charge Q on the capacitor also varies with time. This represents an AC current in the circuit which delivers output power to the load R_L. There is no DC current through the auxiliary power supply V_{in}. Therefore it does not provide the net output power and its lifetime can thus be extended.

2.1. Geometric Design of Variable Capacitor

Figure 2(a) shows a typical layout of the micro generator with in-plane gap-closing capacitor fingers. Whereas the layout can have various forms according to specific design considerations, it can always be lumped as three functional parts: shuttle mass, finger electrodes of the variable capacitor, and mechanical support as shown in Figure 2(b). The mechanical support is related to the structural robustness but does

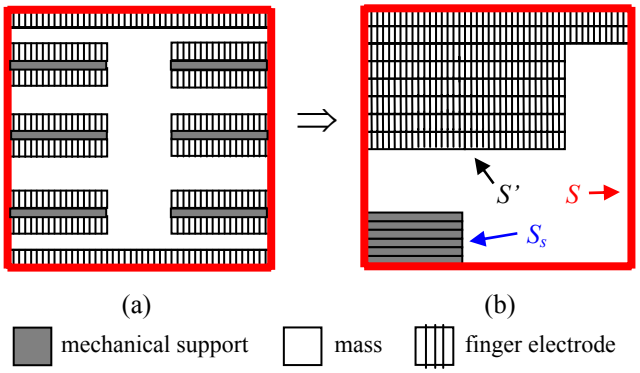

Fig. 2: Area ratio of the capacitor in a typical generator.

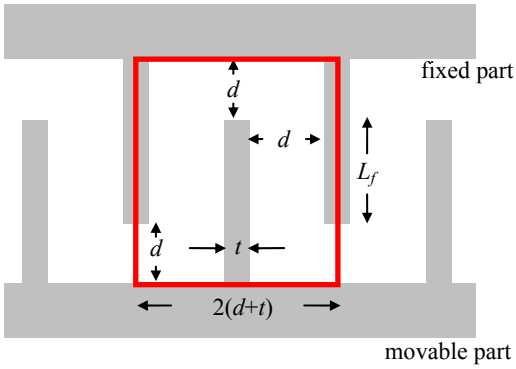

Fig. 3: Unit finger cell in the variable capacitor.

not contribute to the energy conversion. To simplify the discussion, it is not explicitly considered in the optimization in this paper. It is assumed that minimum area is used for mechanical support and adjustment of the resonance frequency of the generator. The area ratio S_r is defined as the percentage of the area occupied by the capacitor fingers in the entire device,

$$S_r = \frac{S'}{(S\text{-}S_s)}, \tag{1}$$

where S is the total device area, S' is the area for the comb fingers of the variable capacitor, and S_s is the area for the mechanical support, as shown in Figure 2(b). In addition to the area ratio, the capacitance also depends on the finger gap d. Figure 3 shows a unit finger cell in the capacitor electrodes where L_f is the finger overlap length, t is the finger width and d is the initial finger gap. The spacing around the finger electrodes is kept constant to avoid the RIE lag and loading effects in the device fabrication. The capacitance C_v can be written as

$$C_v = \frac{2d\varepsilon L_f hN}{d^2 - z^2}, \tag{2}$$

where ε is permittivity of air, h is the finger height, N is the number of fingers, z is the displacement of the shuttle mass with respect to the device frame. From Figure 3 and Eq. 1, the number of fingers and the shuttle mass can be determined as,

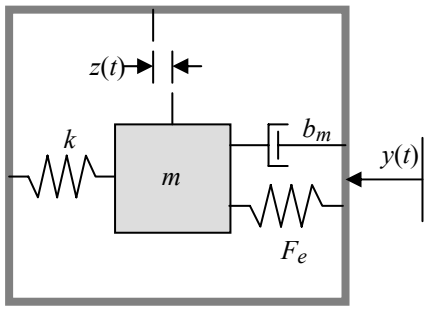

Fig. 4: Schematic of the generator dynamic model.

$$N = \frac{(S - S_s)S_r}{2(d+t)(L_f + 2d)}, \tag{3}$$

$$m = \rho h\left[(S - S_s)(1 - S_r) + Nt(L_f + d)\right] + m_b, \tag{4}$$

where ρ is the mass density of the MEMS substrate and m_b is the mass of the external mass, if any. Once the mass and capacitance are found from the above equations, the system dynamics can be analyzed.

2.2. Equation of Motion

Figure 4 shows the mass-damper-spring model of the generator. The nonlinear equation of motion can be written as

$$m\ddot{z} + b_m\dot{z} + kz = -m\ddot{y} + F_e, \tag{5}$$

where y is the displacement of the device frame caused by the vibration, $b_m\dot{z}$ is the mechanical damping force and F_e is the electrostatic force, which is a function of the electric charge Q on the capacitor according to

$$F_e = \frac{Q^2}{2d\varepsilon L_f hN} z. \tag{6}$$

The time derivative of Q corresponds to the electric current i through the load R_L in Figure 1,

$$i = \dot{Q} = \frac{V_R}{R_L} = \frac{1}{R_L}(V_{in} - \frac{Q}{C_v}). \tag{7}$$

The output power P of the generator and its average P_{av} can be calculated as

$$P = i^2 R_L = \frac{1}{R_L}\left(V_{in} - \frac{Q(d^2 - z^2)}{2d\varepsilon L_f hN}\right)^2, \tag{8}$$

$$P_{av} = \frac{1}{T}\int_0^T P dt. \tag{9}$$

This mathematical model can be used to calculate the output and optimize the device design with respect to various design and operation parameters.

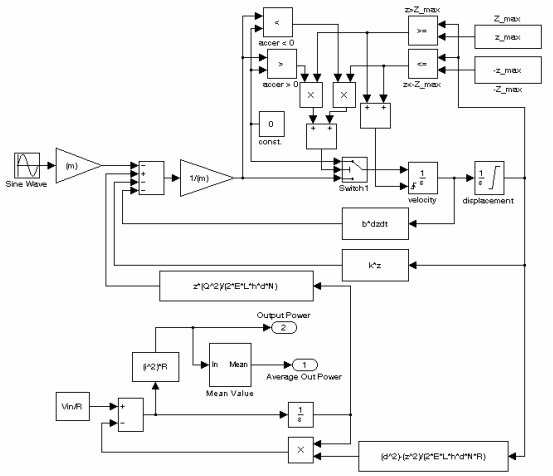

Fig. 5: Simulink block diagram of the generator.

Table 1: Optimization parameters and their range.

	Descriptions	Range
R_L	Load resistance	1 ~ 100 MΩ
S_r	Area ratio	0.025 ~ 0.9
d	Finger initial gap	15 ~ 45 μm

3. SIMULATION AND OPTIMIZATION

The energy converter can be described by three state variables: electric charge Q, displacement z and velocity $\dot{z}$. However, the nonlinear electrostatic force in Eq. 6 makes it difficult to find the steady response analytically. Therefore Eqs. 5 to 7 are transformed into a Simulink model to study the dynamic characteristics of the capacitive micro generator, as shown in Figure 5.

Three parameters, as listed in Table 1, are used to find the optimized device design and operation conditions. The auxiliary power supply V_{in} is 9 volt and the device area is limited to 1 cm^2. Two devices are considered in the analysis. One is without the external mass, the other is with an external mass.

3.1 Without External Mass

Figure 6 shows the simulated output power of a particular device with S_r = 0.1 versus load and initial gap in the range in Table 1. The maximum power and the associated optimal load and initial gap can be found from the local maximum in the plot. Figure 7 shows the maximum power, optimal load and initial finger gap versus S_r. In contrast to the expectation, the output power increases monotonically with decreasing S_r within the range of simulation. The global maximum power of 43.3 nW occurs at the initial gap d = 18 μm, R_L = 88 MΩ and S_r = 0.025 without attached external mass. It is found from the simulation that the amplitude of the oscillation is limited by the side pull-in effect. When S_r increases, the proof mass and its inertial force decrease and become too small to resist the electrostatic force. Therefore the trade-off in S_r is dominated by the mass only and small S_r, thus large

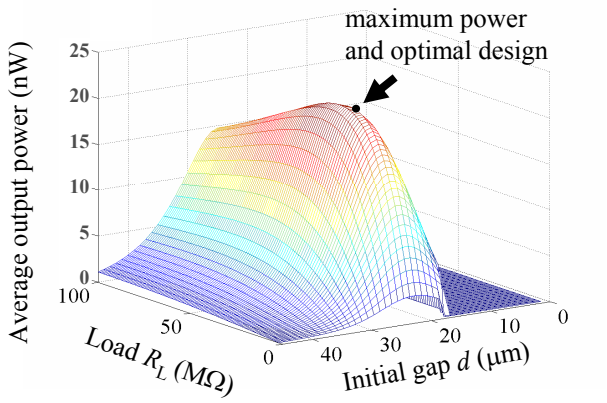

Fig. 6: Average output power for S_r = 0.1 without external mass.

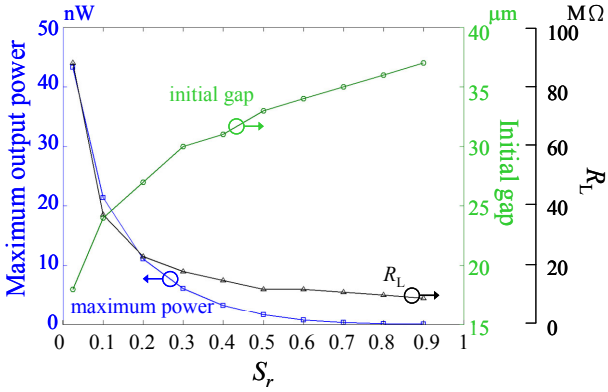

Fig. 7: Maximum output power, initial gap, and optimal load vs. S_r without extermal mass.

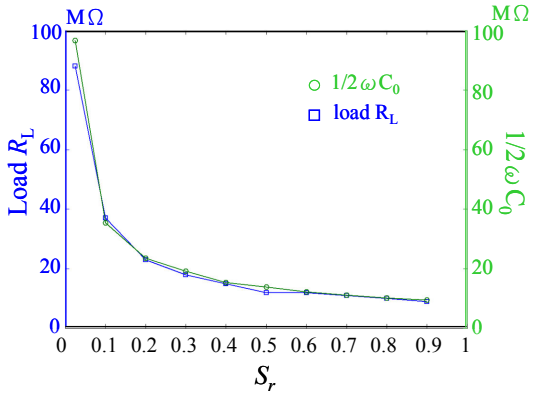

Fig. 8: Optimal load resistance and capacitor impedance vs. S_r.

mass, is favored. The load matching condition is also investigated. Since the capacitance of the symmetric comb electrodes changes at twice the frequency f of the oscillation of shuttle mass, the impedance of the capacitor at rest (z = 0) is calculated at $2f$ and compared to the optimal load R_L in Figure 8. It shows the optimal load R_L is almost identical to the static impedance of the capacitor at rest. This indicates the voltage variation across the variable capacitor caused by the limited oscillation is small enough so that optimal power efficiency can be found at the nominal matched load $R_L = 1/2\,\omega C_0$.

3.2 With 4-gm External Mass

A 4-gm tungsten ball can be attached to the micro generator to increase the output power [2]. Figure 9 shows the simulated output power of a particular device with S_r = 0.5. Figure 10 shows the maximum power, optimal load and initial finger gap versus S_r. Since the total mass in this design is dominated by the external mass, there is no trade-off between mass and capacitor in the layout; therefore the maximum output power is positively correlated to the capacitance and thus S_r. However, increasing S_r implies reduced mass and mechanical strength of the generator. Therefore, S_r is limited to 0.5 in actual design due to the robustness concern of the device when a large external mass is attached. Under this condition, Figure 8 shows the maximum output power of 10.6 μW occurs at the initial gap of 25 μm and load of 2 MΩ. Table 2 summarizes the maximum power and optimal design for the devices with and without the external mass.

4. CONCLUSION

This paper presented the Simulink simulation and optimization of an AC electrostatic micro power generator with 1 cm^2 area constraint. Optimal values were found for the initial finger gap, area ratio, and external load. The micro generator with a 4-gm tungsten ball provides a maximum average output power of 10.6 μW for the initial gap of 25 μm and external load of 2 MΩ. Without the external mass, the generator can produce a maximum average output power of 43.3 nW for the initial gap of 18 μm and external load of 88 MΩ.

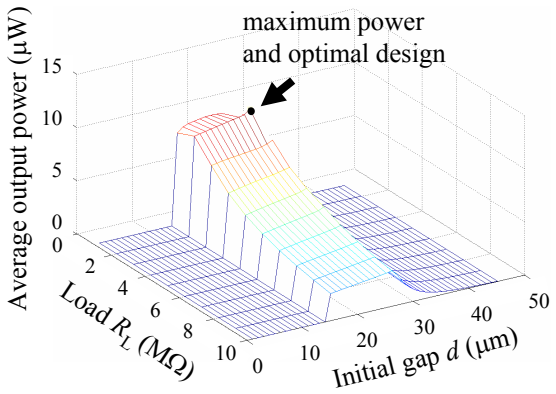

Fig. 9: Average output power for S_r = 0.5 with external mass.

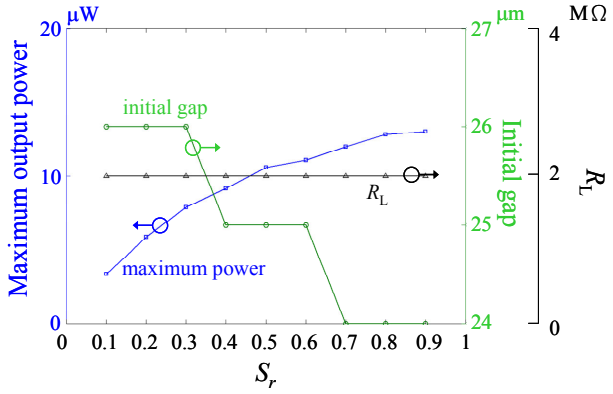

Fig. 10: Maximum output power, initial gap, and optimal load vs. S_r with external mass.

Table 2: Design for maximum output power.

	Without mass	With 4-gm mass
Initial gap d	18 μm	25 μm
Area ratio S_r	0.025	0.5 (limited by structural robustness)
Load resistance R_L	88 MΩ	2 MΩ
Output power P_{max}	43.3 nW	10.6 μW

This project was supported in part by the Ministry of National Science Council, Taiwan, R.O.C., under contract no. NSC 98-2220-E-009-040. The authors were grateful to the use of facilities at the National Center for High-performance Computing and the National Nano Device Laboratory, Taiwan, R.O.C..

REFERENCES

[1] P. D. Mitcheson, T. Sterken, C. He, M. Kiziroglou, E. M. Yeatman and R. Puers, 2008, "Electrostatic microgenerators," *Meas. Control*, **41**, 114-119.

[2] Y. Chiu and V. F. G. Tseng, 2008, "A capacitive vibration-to-electricity energy converter with integrated mechanical switches," *J. Micromech. Microeng.*, **18**, 104004.

[3] S. Roundy and P. K. Wright, 2002, "Micro-electrostatic vibration-to-electricity Converters," *Proc. IMECE 2002,* 39309.

[4] B. C. Yen and J. H. Lang, 2006, "A variable-capacitance vibration-to-electric energy harvester," *IEEE Trans. Circuits and Systems-I,* **53**(2), 288-295.

[5] Y. Sakane, Y. Suzuki, and N. Kasagi, 2008, "The development of a high-performance perfluorinated polymer electret and its application to micro power generationm," *J. Micromech. Microeng.*, **18**, 104011.

[6] I. Kuehne, A. Frey, D. Marinkovic, G. Eckstein, and H. Seidel, 2008, "Power MEMS - a capacitive vibration-to-electrical energy converter with built-in voltage," *Sensors and Actuators A,* **142**, 263-269.

[7] D. Hoffmann, B. Folkmer, and Y. Manoli, 2009, "Fabrication, characterization and modelling of electrostatic micro-generators," *J. Micromech. Microeng.*, **19**, 094001.